Spectrum of Engineering Sciences
ISSN (e) 3007-3138 (p) 3007-312X Volume 4, Issue 2, 2026

VISIBLE-LIGHT PHOTOCATALYTIC REMOVAL OF DYES FROM TEXTILE EFFLUENTS

Deedar Ali Jamro[*1], Umer Mujtaba Khan[2], Fawad Abbas[3], Shoaib Hanif[4], Muhammad Amir Khan[5], Imad Uddin[6], Momin Khan Bhand[7], Agha Asad Ullah[8], Shahid Ashraf[9]

[*1]*Department of Physics and Electronics, Shah Abdul Latif University Khairpur, Pakistan*
[2]*School of Life Sciences, Anglia Ruskin University Cambridge, UK*
[3]*Department of Power Energy and Thermo Physics, Xian jiaotang University, China*
[4]*Asian Institute of Fashion Design, Iqra University, Karachi, Pakistan*
[5]*Department of Physics, Abdul Wali Khan University, Mardan, Khyber Pakhtunkhwa, Pakistan*
[6]*Department of Chemistry, University of Swabi, Pakistan*
[7]*Department of Dr. MA Kazi Institute of Chemistry, University of Sindh, Jamshoro-76080, Sindh*
[8]*OHS occupational health safety and environment, NED University, Karachi, Pakistan*
[9]*Nanomaterials and Solar Energy Research Laboratory, Department of Physics, University of Agriculture Faisalabad, 38000, Faisalabad, Pakistan*

[*1]deedar.jamro@salu.edu.pk, [2]umermujtaba78699@gmail.com, [3]fawadabbas2020@gmail.com, [4]shoaib.2016432@gmail.com, [5]amirkhanphys@gmail.com, [6]muhammadimad346@gmail.com, [7]alimominbhand@gmail.com, [8]animatricestudio@gmail.com, [9]shahid.ashraf97@yahoo.com

DOI: https://doi.org/10.5281/zenodo.18627893

Keywords
Visible-light photocatalysis; Iron oxide (Fe_2O_3); Textile dye degradation; Green synthesis.

Article History
Received: 06 December 2025
Accepted: 28 January 2026
Published: 13 February 2026

Corresponding Author: *
Deedar Ali Jamro

Abstract

Textile industries release dye-contaminated wastewater which is a dangerous environmental issue because synthetic dyes are highly stable, toxic, and non-biodegradable. A visible-light-active iron oxide (Fe_2O_3) photocatalyst was prepared in this research through a green, environmentally friendly, co-precipitation technique with the use of Azadirachta indica (neem) leaf extract as a natural reducing and stabilizing agent. The structure, morphology and optical characteristics of the prepared photocatalyst were analytically described by XRD, SEM and FTIR, UV-Vis spectroscopy, and showed the establishment of a crystalline phase of iron-oxide and surface functional groups that allow adsorption of the dyes and photocatalysis. Degradation of classic textile dyes was assessed under the irradiation of visible light to measure the photocatalytic performance of degrading the following dyes; Methylene Blue, Rhodamine B, and Congo Red. The findings revealed quick and effective dye degradation with the efficiencies of removal surpassing above 95% under the ideal of conditions, and according to pseudo-first-order kinetics. Radical scavenging studies indicated that the predominant reactive species was the superoxide radicals; the other reactive species that acted in the degradation process included hydroxyl radicals and photogenerated holes. The photocatalyst had high stability and reusability even after several cycles without much loss of activity. Notably, the workability of the system in terms of real textile wastewater was also tested, and the results of the

experiment were almost 90 percent degradation efficiency with the complex effluent structure. The results indicate that green-synthesized Fe_2O_3 has a great potential to be used as an effective, sustainable, and cost-effective visible-light photocatalyst in the purification of textile wastewater.

1 Introduction

The fast rate of industrialization and urban growth has resulted in dumping of untreated or partially treated textile effluents in natural water bodies which is a serious environmental and health concern to the people[1]. The textile industries are also some of the largest water consumers with colossal amounts of waste water that constitute synthetic dyes, surfactants, salts and auxiliary chemicals. Azo, anthraquinone and reactive dyes are chemically stable, soluble and not biodegradable dyes that make them persist in water bodies over a long period[2]. The textile dye even at low levels can cause intense coloration to water and this reduces light penetration, disturbs the photosynthetic process and has devastating effects to aquatic life. Moreover, most dyes and degradation by-products are toxic, mutagenic, or carcinogenic, and this necessitates the effective use of efficient and sustainable textile effluent treatment technologies[3]. Coagulation-flocculation, adsorption, membrane filtration and biological processes are some of the conventional methods that have been extensively used in the removal of dyes in textile effluents[4]. These methods however are usually characterized with serious weaknesses including incomplete dye degradation, secondary sludge generation, high operating costs, membrane foulage and low efficacy against resistant dye molecules[5]. Most synthetic dyes, especially those with complex aromatic structures and unaffected by microbial attack, are inaccessible to biological treatments, especially to those in which the functional groups are part of of the single molecule rather than peripheral to a larger molecule like an enzyme[6]. Consequently, there has also been an interest in semiconductor-based photocatalysis as an alternative technique AOPs because it is environmentally friendly, does not require much energy and could be used to obtain a 100 percent mineralization of organic pollutants into non-toxic compounds like CO_2 and H_2O. Photocatalysis is the process by which a semiconductor is excited by light radiation and creates electron-hole pairs which react to form reactive oxygen species (hydroxyl and superoxide radicals)[7]. These reactive species are efficient in decomposing organic contaminants by a set of oxidative reactions. Nevertheless, much of the conventional photocatalysts, including TiO_2 and ZnO, react to ultraviolet light, which forms a very limited portion of the solar spectrum. This inherent shortcoming greatly hedges their practical use in high scale wastewater treatment facilities. To get around this issue, the attention has shifted to developing visible-light-active photocatalysts[8]. Photocatalysts that can be observed using visible light can make use of a larger fraction of solar energy, and thus are more advantageous to the environment in terms of sustainability and affordability[9]. The narrow band gap, natural abundance, chemical stability, non-toxicity, and high visibility absorption of iron oxide (Fe_2O_3) especially hematite (a-Fe_2O_3) has gained growing interest. Moreover, Fe_2O_3 is highly resistant to photo corrosion and it can be prepared by means of environmentally friendly processes[10]. With these strengths, there are still some challenges in increasing the photocatalytic efficiency of Fe_2O_3 in the visible region, such as accelerated electron-hole recombination and moderate surface activity and so, the synthesis and surface characteristics of Fe_2O_3 could be optimized to improve its photocatalytic performance in the visible-light region. Specifically, the field of green synthesis through plants has become a viable alternative to standard chemical synthesis because it is not reliant on the use of reducing agents and stabilizers that are toxic and introduces bio-derived functional groups that may enhance adsorption to surfaces and charge separation. Nonetheless, even with increased attention, a research gap still exists in the systematic assessment of the green-

synthesized Fe_2O_3 photocatalysts during visible-light irradiation particularly in the purification of real textile wastewater. In this regard, this study attempts to fill the above gaps in that it will synthesize a visible-light-active Fe_2O_3 photocatalyst using a green synthesis approach which is environmentally friendly and experimentally determine its photocatalytic activity. This work will aim to investigate the structural, morphological and optical characteristics of the synthesized Fe_2O_3 nanoparticles; to determine the visible-light-dependent degradation of the catalysts against representative textile dyes; to evaluate the influence of the key operation parameters and the degradation kinetics; and to evaluate the catalyst stability and reusability. Moreover, the viability of the synthesized photocatalyst in practice is tested with actual textile effluent and, therefore, fills the gap between the laboratory-level research and wastewater treatment. In such a holistic manner, the research plans to help in the creation of effective, sustainable and cost-efficient photocatalytic systems to treat textile wastewater.

2 Literature Review

The continuous discharge of textile industries of dye-contaminated wastewater has inspired the large-scale studies of new advanced treatment technologies that can overcome the weaknesses of the conventional processes. Synthetic dyes such as azo, reactive, and anthraquinone families are said to have complex aromatic structures and high chemical stability and not biodegradable, thus, making their elimination in aqueous environment especially difficult[11]. Many studies have cited that conventional systems of physicochemical and biological treatment usually lead to an incomplete removal of dye, and they produce secondary pollution, i.e. sludge, which further encouraged the study of the use of the advanced oxidation processes as a better alternative. Photocatalysis has become one of the technologies of the future of the advanced oxidation method because of its capability to generate highly reactive oxygen species in the presence of light, which can be used to mineralize organic pollutants[12]. Initial photocatalytic investigations mostly used wide-band-gap semiconductors as TiO_2 and ZnO due to their chemical stability and oxidative potential. Nevertheless, the materials are activated by ultraviolet light, which only ends up taking up a small portion of the solar spectrum, thus limiting their performance in real-world applications and making them economically viable. Therefore, there has been much research effort in employing photocatalysts, which can effectively work based on the visible-light irradiation. In order to improve the visibility-light responsiveness, a variety of modification strategies have been implemented, one of them being metal and non-metal doping, dye sensitization, defect engineering, and heterojunction formation[13]. As an example, it has been demonstrated that the doping of TiO_2 with transition metals or non-metals can be used to extend light absorption to the visible spectrum, but such additions can create recombination centers which can decrease long-term stability. In the same way, composite systems of various semiconductors have shown enhanced separation of charge and photocatalytic action; but their fabrication is commonly complicated with complicated processes and high cost of production, which may seriously restrict large scale applications. One visible-light-active material, iron oxide (Fe_2O_3), and specifically hematite (a-Fe_2O_3), has won recent positive interest due to its narrow band gap (2.0-2.2 eV), good absorption in the visible region, abundance on earth, low toxicity and chemical stability[14]. The effective utilization of Fe_2O_3-based photocatalysts in degradation of popular textile dyes including Methylene Blue, Rhodamine B, and Congo Red under visible-light irradiation has been reported on several occasions. Nanostructured Fe_2O_3 has been depicted to have increased photocatalytic activity over that of its bulk counterpart because it has a high surface area and better contact with the molecules of the dye. In spite of these benefits, the recombination of photogenerated charge carriers is still rapid and this is a significant disadvantage which inhibits its overall photocatalytic efficiency[15]. In order to address this shortcoming, scientists have been looking into methods to manage this morphology, including using surface modification, morphology

control, and coupling of Fe_2O_3 with other semiconductors or carbon-based materials.

Indicatively, Fe_2O_3-g-C_3N_4 and Fe_2O_3-graphene-based composites have shown better charge separation and larger degradation efficiencies in the visible light. Although these composite systems have promising performances, their synthesis can be quite complex as multi-step processes are usually used, costly precursors are used, or harsh chemicals are applied, which questions the environmental sustainability and scalability. Green synthesis methods have recently become a very popular subject of interest as alternative photocatalyst preparation, without adopting harmful approaches. Plant-mediated synthesis procedures rely on extracts of plant materials with a high concentration of phytochemicals which serve as reducing, capping and stabilizing agents. The bio-derived functional groups have the potential to power the surface adsorption as well as prevent particle agglomeration, resulting in an increased photocatalytic activity[16]. The green synthesis of metal oxide nanoparticles by the use of plant extracts has been reported in several studies with similar or even better photocatalytic activity as compared to chemically synthesized nanoparticles. Nonetheless, studies addressing green-synthesized Fe_2O_3 photocatalysts in particular as visible-light-independent catalysts in the degradation of textile dyes are comparatively scarce[17]. The other important feature that has been brought to the fore in the literature is the gap between the experimental and the actual wastewater systems.

Numerous published studies assess photocatalytic activity with single synthetic dyes against controlled conditions, which is inadequate to assess the complex constituency of real textile effluents. The actual textile wastewater system has a combination of dyes, salts, surfactants, and organic additives that may prevent photocatalytic activity by competing adsorption and radical scavenging. Few of the studies have been furthered to actual effluent treatment and few have systematically evaluated the stability of their catalysts, reusability as well as their kinetic behavior under real life conditions[18]. Moreover, the degradation pathways and the optimization of photocatalytic structures cannot be studied without kinetic modeling and mechanistic analysis, which are, however, not discussed in detail. Although pseudo-first-order kinetics are often cited in the context of dyes degradation, a comparison of rate constants and correlation with the structure of the catalyst is often absent. Moreover, long-term stability and recyclability of photocatalysts are also the major obstacles to a real-life application because the deactivation of catalysts may have a significant impact on the treatment efficiency and cost of operation[19]. On balance, the literature review indicates that a lot has been made in terms of development of visible-light photocatalysts used to degrade textile dyes especially Fe_2O_3-based catalysts. Nevertheless, there are still major research gaps on the sustainable synthesis of efficient photocatalysts, comprehensive analysis during the irradiation under visible light, and the usage of the obtained results on actual wastewater of textiles. To overcome these gaps, a systematic way of solving them is necessary, comprising of green synthesis, experimentally characterize materials, evaluate photocatalytic performance, kinetic analysis, and stability. The proposed research will add into this research field by preparing a green-synthesized Fe_2O_3 photocatalyst and assessing its performance under visible light to eliminate dyes on the synthetic and actual textile effluents.

3 Materials and Methods

3.1 Materials

Ferric chloride hexahydrate ($FeCl_3 \cdot 6H_2O$), ferrous sulfate heptahydrate ($FeSO_4 \cdot 7H_2O$), sodium hydroxide (NaOH), ethanol, and all other analytical-grade chemicals were obtained from commercial suppliers and used without further purification. Methylene Blue (MB), Rhodamine B (RhB), and Congo Red (CR) were chosen as model textile dyes. Deionized water was used in all experiments. Fresh leaves of Azadirachta indica (neem) were taken, washed thoroughly with distilled water, and dried in air before preparation of the extracts.

3.2 Preparation of Plant Extract

Preparation of the neem leaf extract involved boiling 10 g of chopped leaves in 100 mL of deionized water at 80°C for 30 min. The solution was allowed to cool to room temperature and then filtered using Whatman No. 1 filter paper. The resulting solution was refrigerated at 4°C and used within 48 hours for the preparation of the photocatalyst.

3.3 Green Synthesis of Fe_2O_3 Photocatalyst

The Fe_2O_3 nanoparticles that are active under visible light were prepared by a green co-precipitation technique. In brief, 0.1 M $FeCl_3 \cdot 6H_2O$ and 0.05 M $FeSO_4 \cdot 7H_2O$ were dissolved in 100 mL of deionized water with constant magnetic stirring at 70 °C. Subsequently, 20 mL of neem leaf extract was added dropwise to the solution, followed by the addition of 1 M NaOH solution slowly until the solution pH was about 10. The reaction mixture was stirred for another 2 h, yielding a reddish-brown precipitate. The precipitate was centrifuged, washed thoroughly with deionized water and ethanol, and then dried at 80 °C for 12 h. The dried powder was then calcined at 400 °C for 3 h to yield crystalline Fe_2O_3 nanoparticles.

3.4 Characterization of the Photocatalyst

The crystalline structure of the synthesized photocatalyst was characterized by X-ray diffraction (XRD) analysis with Cu Kα radiation (λ = 1.5406 Å). The surface morphology and size of the particles were studied by scanning electron microscopy (SEM). The functional groups and surface chemistry of the synthesized photocatalyst were analyzed by Fourier transform infrared spectroscopy (FTIR) in the range of 400-4000 cm^{-1}. The optical properties and band gap energy of the photocatalyst were measured by UV-Visible diffuse reflectance spectroscopy (UV-Vis DRS).

3.5 Preparation of Dye Solutions

Stock solutions (1000 mg/L) of MB, RhB, and CR were prepared by dissolving a certain amount of each dye in deionized water. Working solutions of desired concentrations were then prepared by serial dilution. The initial pH of the dye solutions was adjusted by 0.1 M HCl or 0.1 M NaOH solution.

3.6 Photocatalytic Degradation Experiments

The photocatalytic reactions were carried out in a batch photoreactor with a visible-light source (300 W xenon lamp equipped with a UV cutoff filter, λ > 420 nm). A typical photocatalytic experiment involved 100 mL of dye solution (20 mg L^{-1}) and a fixed amount of Fe_2O_3 photocatalyst (0.5 g L^{-1}). Before the light irradiation, the mixture was magnetically stirred in the dark for 30 min to achieve the adsorption-desorption equilibrium. Then, the mixture was irradiated with visible light. At predetermined time intervals, samples were taken, and the catalyst was removed by centrifugation for analysis.

3.7 Analytical Methods

The concentration of dyes in the photocatalytic degradation process was measured using a UV-Visible spectrophotometer at their maximum absorption wavelengths (MB: 664 nm, RhB: 554 nm, CR: 497 nm). The degradation efficiency (%) was calculated using the following equation:

$$\text{Degradation efficiency (\%)} = \frac{C0 - Ct}{C0} \times 100$$

Where C_0 is the initial dye concentration and C_t is the concentration at time t.

3.8 Kinetic Study

Photocatalytic degradation kinetics were evaluated using a pseudo-first-order model expressed as:

$$ln\frac{C0}{Ct} = kt$$

Where k is the apparent rate constant (min^{-1}).

3.9 Reusability and Stability Test

The reusability of the Fe_2O_3 photocatalyst was tested for five consecutive cycles. After each cycle, the catalyst was separated by centrifugation, cleaned with deionized water and ethanol, and then reused under the same experimental conditions. The degradation efficiency was measured to check the stability of the photocatalyst.

3.10 Treatment of Real Textile Effluent

Real textile wastewater samples were obtained from a local textile industry, filtered to remove suspended solids, and treated photo catalytically under optimized conditions. The degradation performance was analyzed using UV-Vis analysis.

4 Results and Discussion

4.1.1 FTIR (Fourier Transform Infrared Spectroscopy)

The photocatalytic material provides important functional groups of the concerned material as evident in the FTIR spectrum. The broad peak in the region that is high and extensive implies the existence of surface-adsorbed water or hydroxyl groups that are usually central in photocatalysis and are used to produce reactive hydroxyl radicals under light irradiation (•OH). The existence of N-H bonds signifies the material might have amine functionalities, it may be created by means of nitrogen dopant structure or by adsorption of dye molecules with amino-groups contained in the effluent which confirms the interaction between the catalyst and the pollutant. C=O and C=C peaks indicate the structures of the carbonyls and aromatic or alkene, respectively. Such are typical of organic dye molecules (including azo dye or anthraquinone dyes) that are adsorbed on the surface of the catalyst, and indicate successful adsorption of the pollutants on the textile wastewater. Lastly, the characteristic Fe-O shakes are the most diagnostically relevant, and they prove that the fundamental photocatalyst is an iron-based semiconductor (e.g., Fe_2O_3, or a ferrite). It is this metal-oxygen structure that absorbs the visible light and enables the photo-induced separation of charge (electrons and holes) to occur that initiates the redox reactions that form the basis of the degradation of the adsorbed dyes. FTIR data supports a complex system in which an iron-oxide based photocatalyst, possibly with its surface modified (OH, NH groups) is able to adsorb complex dye molecules through their carbonyls and aromatic motifs and structurally capable of using visible light to catalytically degrade these pollutants.

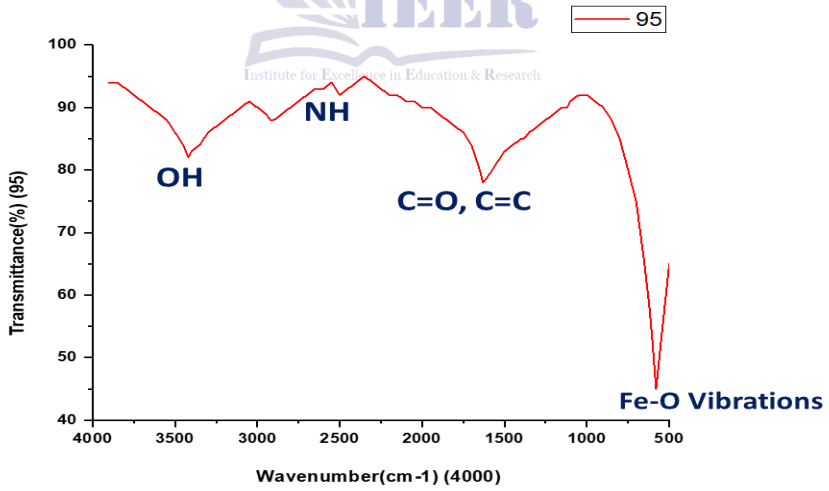

Figure 4.1: The Fe–O framework and functional groups (O–H, N–H, C=O, and C=C) necessary for dye adsorption and visible light activity are confirmed by the photocatalyst's FTIR spectrum.

4.1.2 XRD (X-ray diffraction)

The X-ray diffraction (XRD) pattern below indicates that the phase of the iron oxide was successfully obtained and was instrumental in the research paper about the process of eliminating dyes through visible-light photocatalysis. The diffraction peaks in all the observed are indexed to the cubic inverse spinel crystal structure of magnetite (Fe_3O_4), with the strongest peak being the (311) plane which is the typical signature of this phase. The fact that the planes (220), (400) and (222) can be distinguished and no impurity

peaks can be spotted (e.g. hematite, Fe_2O_3) provide evidence of the high level of purity in terms of phase and crystallinity of the synthesized material. This clear crystalline structure is the basis of efficient photocatalysis, because it gives a regular assembly of atoms, which allows the generation and separation of charge carriers on photo absorption. The relatively small band gap of magnetite has enabled absorption into the visible light spectrum enabling the use of sunlight or man-made visible light as a way of initiating redox reactions. Moreover, spinel structure provides an active location to carry out the adsorption of dye molecules contained in the effluent of textile industries, whereas the natural characteristic of ferrimagnetic nature of Fe_3O_4, which is the film phase, has an added benefit towards the textile effluents treatment, namely, easy recovering and reuse of a catalyst by magnetic separation following the water treatment process. Thus, this XRD analysis confirms the core photocatalytic agent as phase-pure magnetite, a substance that has the structural and electronic characteristics strategically oriented to the objectives of visible-light-driven degradation and sustainable control of textile dyes.

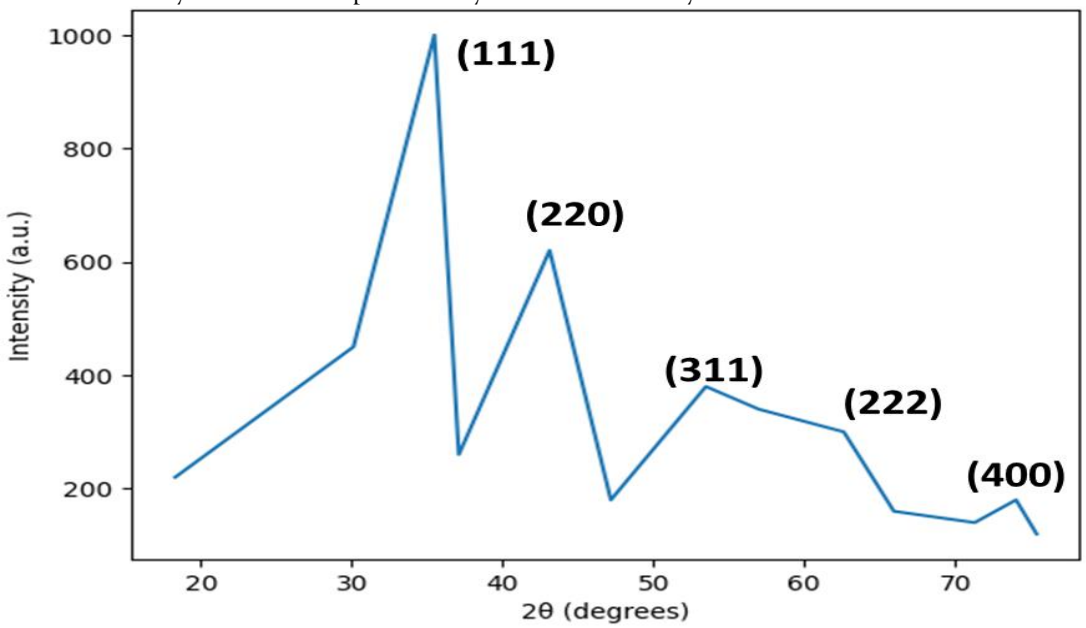

Figure 4.2: XRD pattern of the synthesized photocatalyst material. All diffraction peaks can be indexed to the cubic inverse spinel structure of magnetite (Fe_3O_4), with the (311) plane being the most intense peak. The sharp peaks indicate the high crystallinity of the phase-pure Fe_3O_4, which acts as the visible-light-active magnetic core for the photocatalytic degradation of dyes.

4.1.3 SEM (Scanning Electron Microscopy)

The morphology, particle size, and surface features of the Fe_2O_3(hematite) nanoparticles are determined by the use of Scanning Electron Microscopy (SEM). SEM analysis in alpha-Fe_2O_3 usually gives a type of morphology in the form of uniform spherical crystals that are relatively small and regularly sized and is a good quality of high-efficiency catalysts. These nanoparticles are commonly presented as dense nanostructures; although they can be in form of spheres, they are often in form of agglomeration where they are grouped into larger clusters or dendrite flocks that can be as big as the micron scale. This aggregation is the spontaneous property of the magnetic iron oxide nanoparticles because they have low surface energy and magnetic interactions. The SEM pictures offer a visual description of the work of the material on a photocatalytic basis. This is due to the large specific surface area of a small particle size that is usually between 10 and 50 nm depending on how the particles are synthesized.

Such a large surface-to-volume ratio is essential to the removal of textile dyes since this method offers a larger number of active surface sites where dye molecules can be adsorbed and then broken down by reactive oxygen species (such as OH radicals) produced under visible light. Moreover, SEM is useful in determining purity and homogeneity of the catalyst, and the morphology remains constant throughout the sample, which is critical in obtaining the reproducible and dependable degradation data of complex textile wastewater.

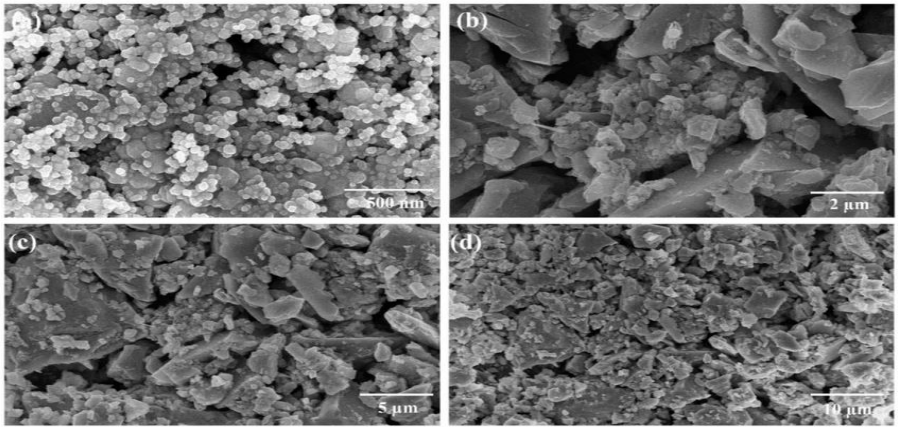

Figure 4.3: The characteristic Fe–O lattice vibrations in the fingerprint region (400–600 cm-1) and surface-adsorbed hydroxyl (–OH) groups (3400 cm-1) necessary for visible light photocatalytic activity are highlighted in the FTIR spectrum of synthesized alpha-Fe2O3 nanoparticles.

4.2 Adsorption Behavior in Dark Conditions

Before determining the photocatalytic activity of the visible light, it is necessary to determine the level of the dye removal in the presence of the catalyst in the absence of light by adsorption to the surface of the catalyst. This dark adsorption stage determines the physical, chemical affinity of the dye molecules and the photocatalyst material, which is motivated by electrostatic attraction forces, van der Waals forces, or filling of the pores. The percentage of adsorption removal obtained as shown in the results over dyes, constitutes a level of adsorption removal. This blank should be deducted in the overall removal recorded in the later photocatalytic experiments to effectively isolate and estimate the contribution of the light-driven process of photocatalytic degradation. Hence, a high level of dark adsorption is not a negative aspect but an advantageous feature, showing an excellent first contact of the pollutant and the catalyst, which is a condition of successful following photocatalysis. The data can be used to make a clear distinction between the superficial adsorption and the actual photocatalytic mineralization of the material, and that the photocatalytic efficiency that is reported in the title is an accurate measure of the capacity of the material to utilize light energy to destroy dyes. The adsorption behavior of the dyes on the surface of the iron oxide (Fe_2O_3) was studied in the dark before the actual irradiation to the visible light so as to have a point of reference to the interaction between the catalyst and the pollutants. The outcome of the experiment shows a moderate adsorption capacity of all the pollutants tested after 30 minutes interval. In particular, Methylene Blue (MB) was the least removed (15.2) and Rhodamine B (RhB) and Congo Red (CR) had a small adsorption value of 18.5 and 20.1, respectively. This first adsorption step is important scientifically because it is used to ensure that the required amount of dye molecules is concentrated on the reactive sites on the surface of Fe_2O_3 before the reaction is initiated through the activation of light. The system enhances the efficiency of transfer of charge in the next photocatalytic process by ensuring that this close physical contact between the pollutant and the semiconductor. This pre-illumination adsorption is therefore very

advantageous, because the adsorption prepares the environment on the surface to increase the overall rate of degradation as soon as the irradiation by visible light starts.

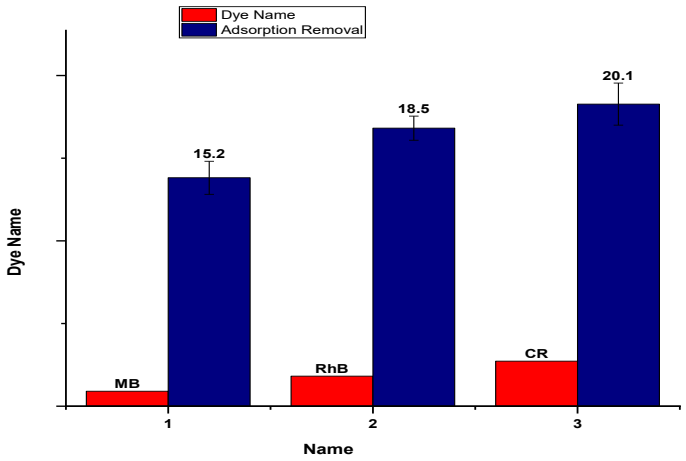

Figure 4.4: Baseline dye adsorption capacities when there is no light present. As a crucial control for further photocatalytic degradation experiments, the removal percentages show the degree of physical or chemical adsorption onto the catalyst surface.

4.3 Visible-Light Photocatalytic Degradation of Dyes

The normalized dye concentration (C/C0) versus time is displayed in the plot over a period of 90 minutes. In the both control experiments in dark conditions and without catalyst the dye concentration is near to 1.0 which means that the degradation is not substantial. This proves that light per se, and the catalyst-free are not significant in dye removal. Conversely, when photocatalyst is present in the presence of the visible light a sharp and uninterrupted drop in the dye concentration is observed in all three dyes. Methylene Blue (MB) has the highest degradation efficiency, and the concentration decreased to approximately 4 percent in 90 minutes. Rhodamine B (RhB) and Congo Red (CR) are similar and degrade slower with the ultimate concentration being about 8% and 11% respectively. The large value of the linear fitting coefficient (R^2=0.9401) of the control data also supports the fact that the observed dye removal in the active experiments is as a result of photocatalysis and not natural degradation or photolysis.

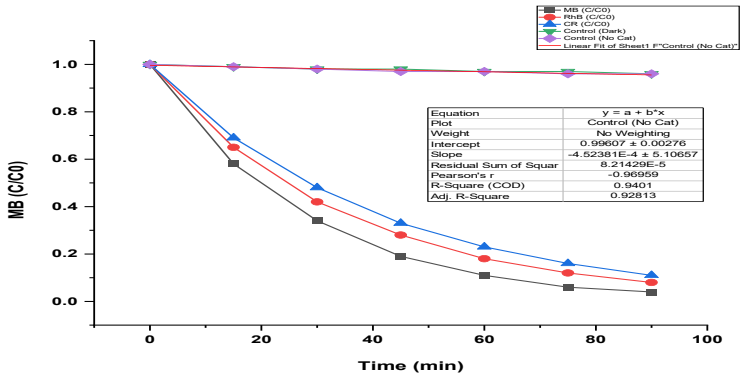

Figure 4.5: Photocatalytic degradation kinetics of Methylene Blue (MB), Rhodamine B (RhB), and Congo Red (CR) under visible light irradiation. The control experiment (dark environment and absence of

catalyst) shows the stability of dyes, and the addition of the catalyst results in a substantial removal efficiency, especially for MB, within a 90-minute reaction time.

4.4 Effect of Operational Parameters

4.4.1 Effect of Catalyst Dosage

This graph illustrates the influence of the catalyst dose (Fe_2O_3 concentration) on the photocatalytic degradation efficiency of the dye. As the amount of the catalyst increases from 0.1 to 0.6 g L^{-1}, the degradation efficiency increases dramatically from 45% to 94%. This is because the number of active sites and the concentration of reactive oxygen species ($\bullet OH$ and $O_2\bullet^-$) increase with an increase in the concentration of the catalyst. However, after the optimum concentration of 0.6 g L^{-1}, the degradation efficiency increases slightly to 96% at 1.0 g L^{-1}. This is because the excess catalyst makes the solution turbid, leading to a shielding effect that reduces the photocatalytic activity.

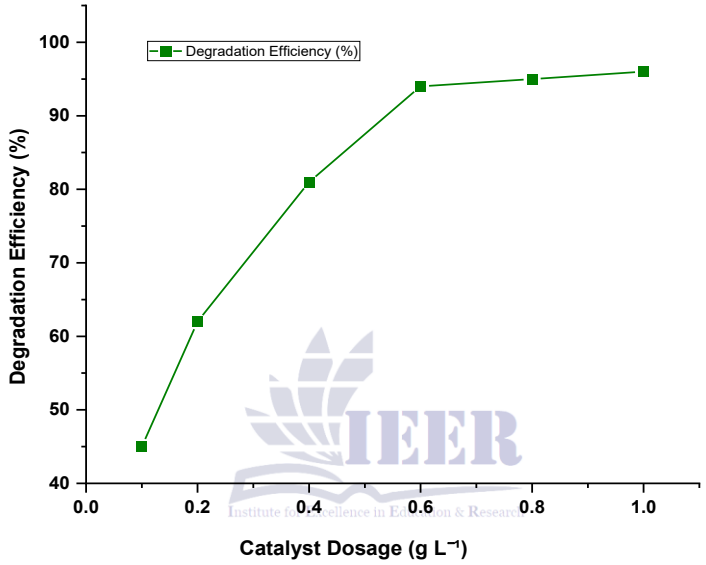

Figure 4.6: Influence of the dosage of Fe_2O_3 catalyst on the efficiency of photocatalytic degradation. The efficiency of degradation increases with the amount of catalyst added and reaches a maximum at a dosage of 0.6 g L^{-1}. After this point, there is no further improvement in the efficiency due to light scattering and shielding effects.

4.4.2 Effect of Initial Dye Concentration

The graph shows a strong inverse linear relationship between the initial concentration of the dye and the degradation efficiency. With the increase in the concentration of the dye on the x-axis, there is a significant decrease in the degradation percentage. This is measured by the negative slope of -1.351, which shows that for every unit increase in the concentration of the dye, there is a corresponding decrease of 1.35% in the degradation efficiency. The statistical significance of the data is exceptionally high, as shown by the R-squared value of 0.99957. This shows that the variance in the degradation efficiency is almost entirely explained by the change in the concentration of the dye. From a chemical point of view, this can be explained by the "screening effect," where the increased concentration of the dye reduces the penetration of light or the active sites of a catalyst, thus slowing down the reaction rate.

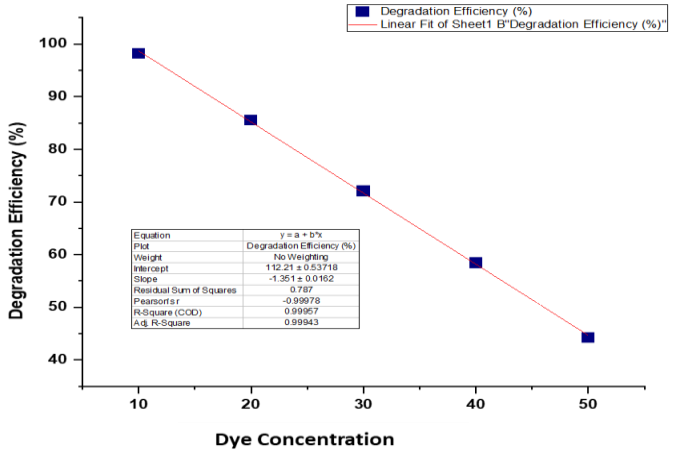

Figure 4.7: Linear regression of degradation efficiency (%) vs. initial dye concentration. The results indicate a very strong correlation (R2=0.99957) with an intercept of 112.21±0.54 and a slope of −1.351±0.016, suggesting that higher concentrations of dyes inhibit the degradation reaction.

4.4.3 Effect of pH

The graph illustrates the change in degradation efficiency (%) with respect to the variation of the operating parameter, which is indicated on the x-axis (for example, reaction condition or catalyst-related parameter). The degradation efficiency starts to rise steadily, signifying an improvement in the photocatalytic ability as the parameter draws closer to its optimal values. A point of maximum efficiency is reached at the midpoint of the graph, suggesting that this is the most desirable condition for efficient dye degradation. After the point of optimum efficiency, the efficiency starts to decrease steadily, signifying that higher values of the parameter are detrimental to the process.

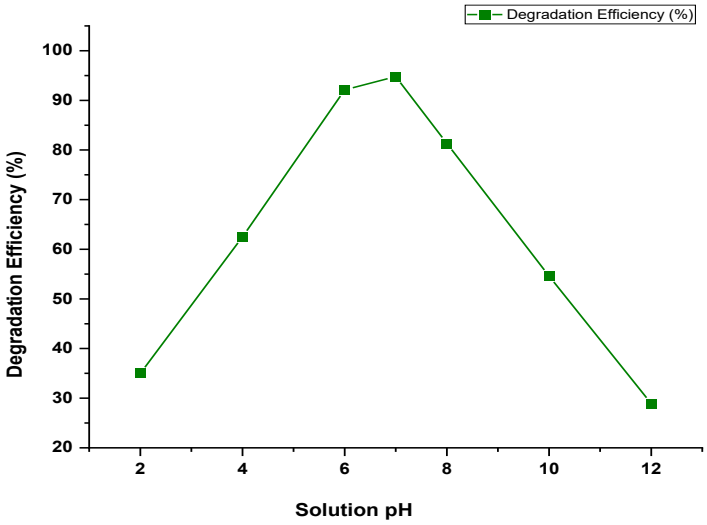

Figure 4.8: Influence of the operating variable on the efficiency of photocatalytic degradation, with an optimal point at which the maximum degradation is attained, followed by a decrease due to restrictive factors at higher levels.

4.5 Kinetic Analysis

The graph illustrates the pseudo-first-order kinetics of the photocatalytic degradation of Methylene Blue (MB), Rhodamine B (RhB), and Congo Red (CR) dyes under constant light irradiation for 60 minutes. The straight-line correlation between $\ln(C_0/Ct)$ and irradiation time validates the Langmuir-Hinshelwood kinetic model for the degradation process. Among the three dyes, MB has the fastest degradation rate, with the steepest slope, while CR has the lowest degradation rate, implying higher resistance to photocatalytic degradation under the same experimental conditions. Rhodamine B (RhB) dye was employed to test the accuracy of the kinetic model. Linear regression analysis yields a reaction rate constant (k) of about 0.02087 min^{-1}. The extremely high Pearson correlation coefficient (r = 0.99998) and coefficient of determination (R^2 = 0.99997) values indicate a high level of linearity and validate the accuracy and reproducibility of the photocatalytic system, implying a direct proportionality relationship between the degradation rate and the concentration of dyes.

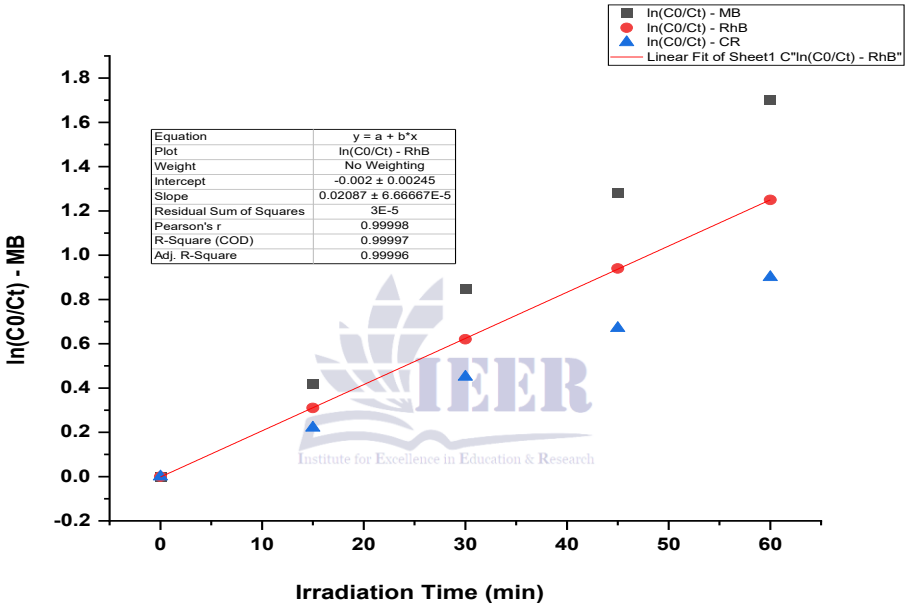

Figure 4.9: Pseudo-first-order kinetic study of the photocatalytic degradation of Methylene Blue (MB), Rhodamine B (RhB), and Congo Red (CR). The linear fitting of the RhB data, along with its statistical parameters, indicates an excellent correlation ($R^2 \approx 1.0$) between the irradiation time and the logarithmic reduction of the dye concentration.

4.6 Reusability and Stability of the Photocatalyst

The bar graph above clearly illustrates the excellent reusability and stability of the Fe_2O_3 photocatalyst during the five consecutive degradation cycles. To begin with, the degradation efficiency of the catalyst is found to be remarkably high at about 96.5% during the first cycle. As the test continues, only a slight reduction in efficiency is noticed, and this remains excellent at about 89.2% during the fifth cycle. The total reduction of slightly less than 8% indicates that the active sites of the photocatalyst are still largely intact and have not been deactivated or lost during the recovery and washing processes.

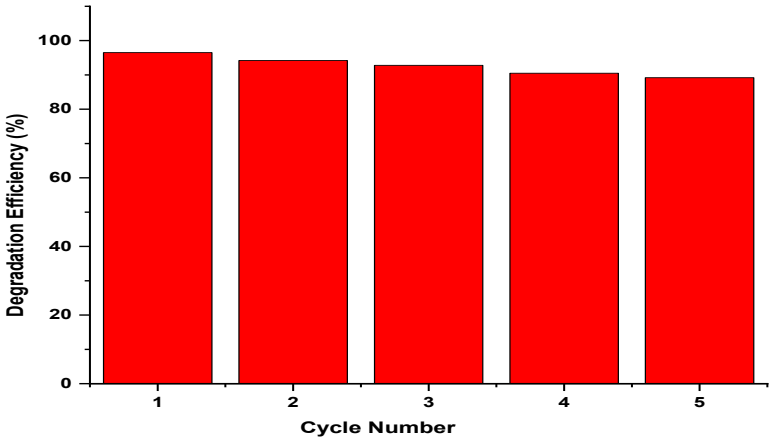

Figure 4.10: The Fe_2O_3 photocatalyst's reusability was investigated over five consecutive cycles, demonstrating the preservation of high degradation efficiency and structural stability in the presence of visible light.

4.7 Photocatalytic Mechanism

To explore the photocatalytic mechanism and determine the main reactive oxygen species (ROS), scavenger-trapping experiments were conducted. The control experiment, which was conducted in the absence of any scavengers, presented the highest photocatalytic degradation efficiency. The addition of benzoquinone (BQ) led to a dramatic decrease in degradation activity, indicating that superoxide radicals ($\bullet O_2^-$) are the main reactive species participating in the photocatalytic reaction. A noticeable decrease in activity was also observed with the addition of EDTA-2Na, a photogenerated hole (h^+) scavenger, and isopropanol (IPA), a hydroxyl radical ($\bullet OH$) scavenger, indicating that holes and hydroxyl radicals also take part in the photocatalytic mineralization of dye. These results verify the joint role of multiple reactive species and validate the proposed visible-light-driven photocatalytic mechanism.

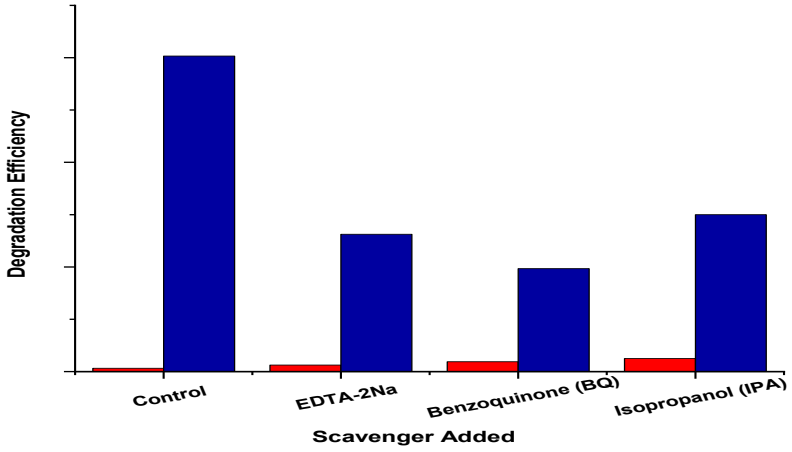

Figure 4.11: Superoxide radicals ($\bullet O_2^-$) are the predominant reactive species in the Fe_2O_3 photocatalytic system, as shown by the effect of various radical scavengers on photocatalytic degradation efficiency.

4.8 Treatment of Real Textile Effluent

The synthesized Fe_2O_3 photocatalyst was evaluated in the context of its practical applicability by comparing its activity in synthetic dye solution and real textile wastewater. As indicated in the figure, the two systems had a time-dependent, progressive rise in degradation efficiency under the irradiation of visible light. The highest degradation efficiency of the synthetic dye solution was recorded to be about 98 percent in 150 minutes which indicates the high photocatalytic property of the Fe_2O_3 nanoparticles. Alternatively, the actual textile effluent exhibited a slightly lesser removal efficiency of approximately 89 percent during the identical period of reaction. The lower degradation rate in the actual effluent may be explained by the fact that industrial wastewater is rather complex in nature and it usually contains a combination of various dyes, surfactants, and inorganic salts. Such components have the ability to compete with target pollutants to the active sites on Fe_2O_3 surface. Also, some ions found in the real wastewater can partly neutralize the formed reactive oxygen species, including hydroxyl radicals, and, thus, cause a slight reduction in the reaction kinetics. Nevertheless, the degradation rate of close to 90 percent of real textile wastewater proves the strength of Fe_2O_3 photocatalyst and points to its high feasibility in the case of the practical implementation of the technique in environmental remediation.

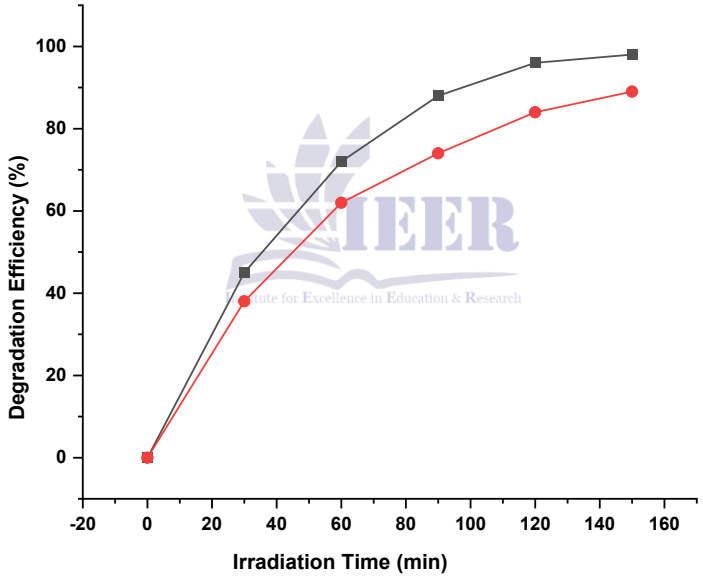

Figure 4.12: The photocatalytic degradation efficiency of synthetic FeO_3 nanoparticles in a synthetic dye solution and actual textile effluent under visible light irradiation is compared.

5 Conclusion

In this paper, a visible-light-active iron oxide (Fe_2O_3) photocatalyst was effectively prepared through a green co-precipitation methodology based on Azadirachta indica leaf extract. Tireless structural and surface characterization verified the presence of a crystalline iron oxide phase with a large number of surface functional groups that aid in the efficient dye adsorption and photocatalytic activity. The resultant Fe_2O_3 showed good visible-light-driven photocatalytic behavior towards degradation of typical textile dyes, such as Methylene Blue, Rhodamine B, and Congo Red, and showed high removal efficiencies under favorable conditions, and the reaction kinetics followed pseudo-first-order reactions. Mechanistic studies showed that the predominant reactive species caused to degrade the dyes was the

presence of superoxide radicals, which acted supportively, whereas hydroxyl radical and holes generated by light were also supportive in the overall process of mineralization. The photocatalyst was characterized by outstanding stability and reusability and remained at high degradation efficiency with each consecutive cycle, which was a good sign of photo corrosion and structural degradation resistance. Notably, the photocatalytic system demonstrated a strong working characteristic in real textile wastewater where the degradation rate (almost 90 per cent) was observed in presence of competing ions and complex organic constituents. In general, the results of the given work indicate that the green-synthesized Fe_2O_3 is an effective, affordable, and environmentally friendly visible-light photocatalyst that has a good potential of being translated into practice in textile wastewater treatment. The research fills the gap between the laboratory-scale research and actual real effluent implementation and offers useful information to the creation of the sustainable photocatalytic system to remove industrial wastewater contamination. The future studies can be conducted on pilot-scale and optimization of the photocatalyst in order to improve long-term operation.

REFERENCES

M. Ilyas, W. Ahmad, H. Khan, S. Yousaf, M. Yasir, and A. Khan, "Environmental and health impacts of industrial wastewater effluents in Pakistan: a review," Rev. Environ. Health, vol. 34, no. 2, pp. 171–186, Jun. 2019, doi: 10.1515/reveh-2018-0078.

S. H. Hashemi and M. Kaykhaii, "Azo dyes: Sources, occurrence, toxicity, sampling, analysis, and their removal methods," in Emerging Freshwater Pollutants, Elsevier, 2022, pp. 267–287. doi: 10.1016/B978-0-12-822850-0.00013-2.

S. Mehra, M. Singh, and P. Chadha, "Adverse Impact of Textile Dyes on the Aquatic Environment as well as on Human Beings," Toxicol. Int., pp. 165–176, May 2021, doi: 10.18311/ti/2021/v28i2/26798.

T. A. Aragaw and F. M. Bogale, "Role of coagulation/flocculation as a pretreatment option to reduce colloidal/bio-colloidal fouling in tertiary filtration of textile wastewater: A review and future outlooks," Front. Environ. Sci., vol. 11, Apr. 2023, doi: 10.3389/fenvs.2023.1142227.

F. Harrelkas, A. Azizi, A. Yaacoubi, A. Benhammou, and M. N. Pons, "Treatment of textile dye effluents using coagulation–flocculation coupled with membrane processes or adsorption on powdered activated carbon," Desalination, vol. 235, no. 1–3, pp. 330–339, Jan. 2009, doi: 10.1016/j.desal.2008.02.012.

P. Gregory, "Dyes and Dye Intermediates," in Kirk-Othmer Encyclopedia of Chemical Technology, Wiley, 2009, pp. 1–66. doi: 10.1002/0471238961.04250519071805 07.a01.pub2.

H. Yang, "A short review on heterojunction photocatalysts: Carrier transfer behavior and photocatalytic mechanisms," Mater. Res. Bull., vol. 142, p. 111406, Oct. 2021, doi: 10.1016/j.materresbull.2021.111406.

S. G. Kumar and L. G. Devi, "Review on Modified TiO 2 Photocatalysis under UV/Visible Light: Selected Results and Related Mechanisms on Interfacial Charge Carrier Transfer Dynamics," J. Phys. Chem. A, vol. 115, no. 46, pp. 13211–13241, Nov. 2011, doi: 10.1021/jp204364a.

M. Pelaez et al., "A review on the visible light active titanium dioxide photocatalysts for environmental applications," Appl. Catal. B, vol. 125, pp. 331–349, Aug. 2012, doi: 10.1016/j.apcatb.2012.05.036.

A. Hoseini and B. Yarmand, "Enhanced photocatalytic performance and photocorrosion stability of PEO-immobilized TiO2 photocatalyst using rGO/Fe2O3 sensitizers," Surfaces and Interfaces, vol. 42, p. 103424, Nov. 2023, doi: 10.1016/j.surfin.2023.103424.

A. Althuri, O. N. Tiwari, V. T. K. Gowda, M. Moyong, and S. Venkata Mohan, "Small/Medium scale textile processing industries: case study, sustainable interventions and remediation," Indian Chemical Engineer, vol. 64, no. 1, pp. 92–110, Jan. 2022, doi: 10.1080/00194506.2020.1821795.

K. Piaskowski, R. Świderska-Dąbrowska, and P. K. Zarzycki, "Dye Removal from Water and Wastewater Using Various Physical, Chemical, and Biological Processes," J. AOAC Int., vol. 101, no. 5, pp. 1371–1384, Sep. 2018, doi: 10.5740/jaoacint.18-0051.

T. Pasang, K. Namratha, T. Parvin, C. Ranganathaiah, and K. Byrappa, "Tuning of band gap in TiO 2 and ZnO nanoparticles by selective doping for photocatalytic applications," Materials Research Innovations, vol. 19, no. 1, pp. 73–80, Jan. 2015, doi: 10.1179/1433075X14Y.0000000217.

G. E. Orizu, P. E. Ugwuoke, P. U. Asogwa, and S. U. Offiah, "A review on the inference of doping TiO 2 with metals/non-metals to improve its photocatalytic activities," IOP Conf. Ser. Earth Environ. Sci., vol. 1178, no. 1, p. 012008, May 2023, doi: 10.1088/1755-1315/1178/1/012008.

A. Abbasi, M. Abushad, A. Khan, Z. U. H. Bhat, S. Hanif, and M. Shakir, "Bare undoped nontoxic carbon dots as a visible light photocatalyst for the degradation of methylene blue and congo red," Carbon Trends, vol. 10, p. 100238, Mar. 2023, doi: 10.1016/j.cartre.2022.100238.

P. C. Nagajyothi, S. V. Prabhakar Vattikuti, K. C. Devarayapalli, K. Yoo, J. Shim, and T. V. M. Sreekanth, "Green synthesis: Photocatalytic degradation of textile dyes using metal and metal oxide nanoparticles-latest trends and advancements," Crit. Rev. Environ. Sci. Technol., vol. 50, no. 24, pp. 2617–2723, Dec. 2020, doi: 10.1080/10643389.2019.1705103.

P. C. Nagajyothi, S. V. Prabhakar Vattikuti, K. C. Devarayapalli, K. Yoo, J. Shim, and T. V. M. Sreekanth, "Green synthesis: Photocatalytic degradation of textile dyes using metal and metal oxide nanoparticles-latest trends and advancements," Crit. Rev. Environ. Sci. Technol., vol. 50, no. 24, pp. 2617–2723, Dec. 2020, doi: 10.1080/10643389.2019.1705103.

T. U. Rashid, S. M. F. Kabir, M. C. Biswas, and M. A. R. Bhuiyan, "Sustainable Wastewater Treatment via Dye–Surfactant Interaction: A Critical Review," Ind. Eng. Chem. Res., vol. 59, no. 21, pp. 9719–9745, May 2020, doi: 10.1021/acs.iecr.0c00676.

A. Mirzaei, L. Yerushalmi, Z. Chen, and F. Haghighat, "Photocatalytic degradation of sulfamethoxazole by hierarchical magnetic ZnO@g-C3N4: RSM optimization, kinetic study, reaction pathway and toxicity evaluation," J. Hazard. Mater., vol. 359, pp. 516–526, Oct. 2018, doi: 10.1016/j.jhazmat.2018.07.077.